

## Analytical solutions of in-plane static problems for non-uniform curved beams including axial and shear deformations

Ekrem Tufekci<sup>†</sup> and Alaeddin Arpacı<sup>‡</sup>

*Istanbul Technical University, Faculty of Mechanical Engineering, Gumussuyu 34437, Istanbul, Turkey*

*(Received July 28, 2004, Accepted October 24, 2005)*

**Abstract.** Exact analytical solutions for in-plane static problems of planar curved beams with variable curvatures and variable cross-sections are derived by using the initial value method. The governing equations include the axial extension and shear deformation effects. The fundamental matrix required by the initial value method is obtained analytically. Then, the displacements, slopes and stress resultants are found analytically along the beam axis by using the fundamental matrix. The results are given in analytical forms. In order to show the advantages of the method, some examples are solved and the results are compared with the existing results in the literature. One of the advantages of the proposed method is that the high degree of statically indeterminacy adds no extra difficulty to the solution. For some examples, the deformed shape along the beam axis is determined and plotted and also the slope and stress resultants are given in tables.

**Key words:** curved beam; variable cross-section; axial extension; shear deformation; initial value method.

---

### 1. Introduction

Many engineering structures can be modeled as beam elements. Arch elements occur frequently in many engineering applications such as spring design, electrical machinery, turbo-machinery blades, circumferential stiffeners for shells, aerospace structures, arch bridges, highway construction, long span roof structures and earthquake resistant structures. Considerable amount of attention has been devoted to the analysis of such elements, in recent years. In-plane behavior of a curved beam possesses axial extension as well as flexural deformation. The initial curvature introduces geometric coupling between the axial and bending deformations. The analysis of curved beams is quite complex due to the presence of coupling between these deformations.

One of the most important studies on the theory of elasticity of curved beams belongs to Love (1944). The early works of Kirchhoff and Euler who analyzed large deformations of elastic beams in equilibrium is discussed in the book by Love (1944). The general governing equations for a spatial curved beam were given in scalar quantities. The reference curve of the beam is inextensible

---

<sup>†</sup> Assistant Professor, Corresponding author, E-mail: [tufekcie@itu.edu.tr](mailto:tufekcie@itu.edu.tr)

<sup>‡</sup> Professor, E-mail: [arpacial@itu.edu.tr](mailto:arpacial@itu.edu.tr)

and the effect of tangential shear deformation is neglected.

The interaction between axial force and bending moment was considered by Asplund (1961). The displacements based on the original geometry were computed by a method of successive approximation and the displacements were used to obtain the geometry.

The in-plane deformation of a curved beam subjected to concentrated and/or distributed loads can be characterized by a system of 6 coupled ordinary differential equations, resulting in a complicated two-point boundary value problem. However, this problem can be converted to an initial value problem and a variety of existing computer programs can be used to integrate the equations. One of the early applications of the conversion of a boundary value problem to an initial value problem for curved beams is found in Huddleston (1968).

Antman (1972) studied the problems that help clarify the structure of nonlinear continuum mechanics, employing linear theories in some examples. The analysis of equilibrium of beams has been generalized by including the effects of extension of the beam axis and tangential shear deformation. Several rational developments of beam theories and the corresponding diverse interpretations of the role and scope of such theories were examined. A variety of problems in the theory of nonlinearly elastic beams were also treated.

Cinemre (1982) obtained the strain-displacement relations geometrically, where the beam is represented as a directed space curve and the restrictions of perpendicular cross-section to the tangent of the space curve and inextensible arch length are removed, in contrast with Kirchhoff's beam theory. The displacement of a point on the space curve and the rotation of the cross-section constitute the displacement field of the beam. The change in the tangent vector from the initial state and the rate of change vector of the deformed director diad are chosen to represent the state of strain.

Rubin (2000) represented a unified approach to the development of the Cosserat theories which are three-dimensional theory, two-dimensional shell theory, one-dimensional beam theory and zero-dimensional point theory. The beam theory allows the deformation of a beam to be arbitrary. The cross-section does not have to be normal to the beam axis. The beam is said to have experienced normal cross-sectional extension when the dimensions of the cross-section change, tangential shear deformation when the cross-section is not normal to the deformed beam axis, and normal cross-sectional shear deformation when the angle between the directors of the cross-section changes.

It is often difficult and sometimes impossible to solve a curved beam problem exactly. Castigliano's method, the Rayleigh-Ritz method, the Galerkin method and the differential quadrature method have been used to predict the static behavior of a curved beam based on the Euler-Bernoulli and Timoshenko beam theories. Most of the theoretical works included the application of various numerical methods to solve the problems of curved beams. It seems that the finite elements have been the major tool in these studies. Several special elements for curved geometry have been developed. Some of the elements are based on the nonlinear beam theories. Reissner's finite strain beam theory (Reissner 1972, 1973) is the most important one. In particular, the formulation of finite elements for curved beams has been the subject of intensive research interest. Early attempts to formulate a curved finite beam element were unsuccessful and resulted in inaccurate element formulations. In a curved beam, both shear locking and membrane locking take place when the beam is modeled by the lower-order conventional curved beam elements. Much attention has been focused to remedy the locking over the years, since the locking concept was first introduced into this field. Several methods have been proposed to alleviate the locking phenomena. Some of the methods are the selective/reduced integration (Stolarski and Belytschko 1983), higher order

interpolations (Dawe 1974), shear penalty relaxation method (Tessler and Spiridigliozzi 1986), field consistency (Atluri *et al.* 2001), and hybrid/mixed formulations (Benlemlih and El Ferrichia 2002, Kim and Kim 1998).

The shallow curved beam is one of the simplest structures exhibiting the important features associated with elastic instability. The structure suddenly jumps from one stable equilibrium configuration to another one or after exceeding a certain load level, the structure deforms along a secondary path representing an asymmetric mode (Tufekci 2001, Rubin 2004). A number of finite elements have been developed for analyzing the shallow beam problems (Stolarski and Belytschko 1983, Schulz and Filippou 2001, Dawe 1974).

The foregoing review has shown that most of the papers deal with uniform circular beams and none of them provides analytical expressions for the displacements and stress resultants of curved beams having variable curvature and variable cross-section. Some of the papers employ analytical methods by neglecting the axial and shear deformations. Numerical methods have been widely used in the analyses, and the finite element methods have been the major tool in the analyses of curved beams. There is no curved beam finite element with variable cross-section. The finite element method solves the problems of curved beams with variable cross-section by using piecewise constant cross-section beam elements to approximate the variable cross-section beams. Motivated by this fact, the exact analytical solution of in-plane static problems for a curved beam with variable curvature and variable cross-section is obtained in the present study. The cross-section of the beam is doubly symmetric and the symmetry plane is also the plane of initial curvature, then the in-plane and out-of-plane deformations will be uncoupled. The beam axis can be of any geometry such as a parabola, catenary, cycloid, circle etc. The axial extension and shear deformation effects are considered in the governing differential equations. The strains in the beam are assumed to be small and the stress-strain relation is assumed to be linear. Plane sections remain plane after deformation but not necessarily perpendicular to the beam axis. The disturbed states of deformation at the loading points and boundaries are not taken into account. By using the methodology followed in this paper, it is also possible to study deep and shallow curved beams or thin and thick curved beams without any additional effort.

## 2. Analysis

The extensional, flexural and shear strain components in the polar coordinate system are;

$$\varepsilon_t = \frac{dw}{ds} - \frac{u}{R}, \quad \chi = \frac{d\Omega_b}{ds}, \quad \gamma = \frac{du}{ds} + \frac{w}{R} - \Omega_b \quad (1)$$

where  $u$  and  $w$  are respectively the normal and tangential displacements;  $\Omega_b$  is the rotation angle about the bi-normal axis;  $s$  is the arch length;  $R$  is the radius of curvature of the beam. The constitutive equations are given for an infinitesimal curved beam element as follows;

$$\frac{F_t}{EA} = \varepsilon_t; \quad \frac{M_b}{EI_b} = \chi; \quad \frac{F_n}{k_n GA} = \gamma \quad (2)$$

where  $F_n$  and  $F_t$  are respectively normal and tangential components of internal force;  $M_b$  is the internal moment about the bi-normal axis;  $E$  and  $G$  are respectively Young's and shear moduli;  $A$  is the cross-sectional area;  $I_b$  is the area moment of inertia of the cross-section with respect to the bi-

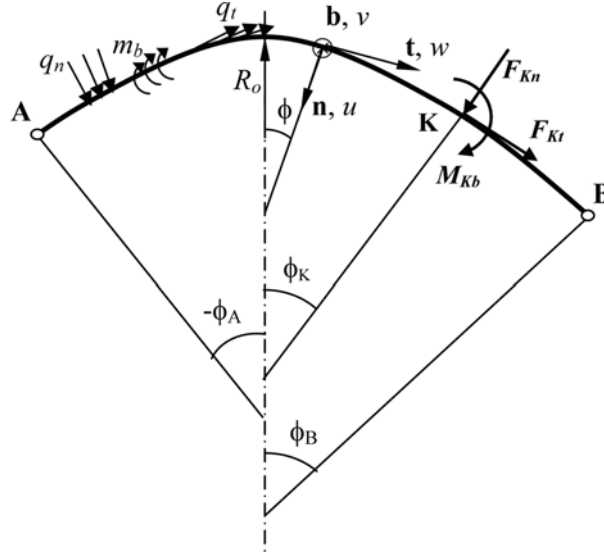


Fig. 1 Schematic view of a planar curved beam considered in this study

normal axis;  $k_n$  is the factor of shear distribution along the normal axis.

The equilibrium equations for an infinitesimal curved beam element are as follows:

$$\frac{dM_b}{ds} + F_n + m_b = 0 \quad \frac{dF_t}{ds} - \frac{F_n}{R} + q_t = 0 \quad \frac{dF_n}{ds} + \frac{F_t}{R} + q_n = 0 \quad (3)$$

where  $q_n$  and  $q_t$  are respectively normal and tangential components of external distributed force; and  $m_b$  is the external distributed moment about bi-normal axis.

The governing differential equations of in-plane behavior of a curved beam (Fig. 1) can be rewritten by using  $ds = R(\phi)d\phi$  as follows:

$$\begin{aligned} \frac{dw}{d\phi} &= u + \frac{R(\phi)}{EA(\phi)} F_t & \frac{du}{d\phi} &= -w + \frac{R(\phi)}{k_n GA(\phi)} F_n + R(\phi) \Omega_b \\ \frac{d\Omega_b}{d\phi} &= \frac{R(\phi)}{EI_b(\phi)} M_b & \frac{dM_b}{d\phi} &= -R(\phi) F_n - R(\phi) m_b \\ \frac{dF_t}{d\phi} &= F_n - R(\phi) q_t & \frac{dF_n}{d\phi} &= -F_t - R(\phi) q_n \end{aligned} \quad (4)$$

The governing differential equations of free vibration of a circular beam can be obtained from these equations by using d'Alembert's principle (Tufekci and Arpaci 1998).

The equations can be written in the matrix form:

$$\frac{d\mathbf{y}}{d\phi} = \mathbf{A}(\phi)\mathbf{y} + \mathbf{f}(\phi) \quad (5)$$

where  $\mathbf{y}$  is the vector of variables,  $\mathbf{A}(\phi)$  is the  $6 \times 6$  coefficient matrix and  $\mathbf{f}(\phi)$  is the resultant vector of external distributed loads.

If a beam with concentrated forces and moments is considered, taking  $\mathbf{f}(\phi)$  to be zero, the Eq. (5) reduces to a homogeneous system. The solution vector can be expressed as;

$$\mathbf{y}(\phi) = \mathbf{Y}(\phi, \phi_o)\mathbf{y}_o \quad (6)$$

The fundamental matrix  $\mathbf{Y}(\phi, \phi_o)$  is obtained by solving Eq. (6) and satisfies the following requirements:

$$\begin{aligned} \frac{d\mathbf{Y}(\phi, \phi_o)}{d\phi} &= \mathbf{A}(\phi)\mathbf{Y}(\phi, \phi_o), & \mathbf{Y}(\phi_o, \phi_o) &= \mathbf{I} \\ \mathbf{Y}(\phi_1, \phi_2)\mathbf{Y}(\phi_2, \phi_3) &= \mathbf{Y}(\phi_1, \phi_3), & \mathbf{Y}(\phi_1, \phi_2) &= \mathbf{Y}^{-1}(\phi_2, \phi_1) \end{aligned} \quad (7)$$

where  $\mathbf{I}$  is unit matrix. The solutions of the Eqs. (4) are:

$$F_t = F_{t_o}\cos\phi + F_{n_o}\sin\phi \quad (8)$$

$$F_n = -F_{t_o}\sin\phi + F_{n_o}\cos\phi \quad (9)$$

$$M_b = M_{b_o} + \int_0^\phi R(\psi)\sin\psi d\psi F_{t_o} - \int_0^\phi R(\psi)\cos\psi d\psi F_{n_o} \quad (10)$$

$$\Omega_b = \Omega_{b_o} + \int_0^\phi \frac{R(\psi)}{EI_b(\psi)} d\psi M_{b_o} + \int_0^\phi \frac{R(\psi)}{EI_b(\psi)} \int_0^\psi R(\xi)\sin\xi d\xi d\psi F_{t_o} - \int_0^\phi \frac{R(\psi)}{EI_b(\psi)} \int_0^\psi R(\xi)\cos\xi d\xi d\psi F_{n_o} \quad (11)$$

$$\begin{aligned} u &= -\sin\phi w_o + \cos\phi u_o + \left[ \sin\phi \int_0^\phi R(\psi)\sin\psi d\psi + \cos\phi \int_0^\phi R(\psi)\cos\psi d\psi \right] \Omega_{b_o} \\ &+ \left[ \sin\phi \int_0^\phi R(\psi)\sin\psi \int_0^\psi \frac{R(\xi)}{EI_b(\xi)} d\xi d\psi + \cos\phi \int_0^\phi R(\psi)\cos\psi \int_0^\psi \frac{R(\xi)}{EI_b(\xi)} d\xi d\psi \right] M_{b_o} \\ &+ \left\{ -\sin\phi \int_0^\phi R(\psi) \left[ \frac{\cos^2\psi}{EA(\psi)} + \frac{\sin^2\psi}{k_n GA(\psi)} - \sin\psi \int_0^\psi \frac{R(\xi)}{EI_b(\xi)} \int_0^\xi R(\theta)\sin\theta d\theta d\xi \right] d\psi \right. \\ &+ \left. \cos\phi \int_0^\phi R(\psi)\cos\psi \left[ \frac{\sin\psi}{EA(\psi)} - \frac{\cos\psi}{k_n GA(\psi)} + \int_0^\psi \frac{R(\xi)}{EI_b(\xi)} \int_0^\xi R(\theta)\sin\theta d\theta d\xi \right] d\psi \right\} F_{t_o} \\ &+ \left\{ \cos\phi \int_0^\phi R(\psi) \left[ \frac{\sin^2\psi}{EA(\psi)} + \frac{\cos^2\psi}{k_n GA(\psi)} - \cos\psi \int_0^\psi \frac{R(\xi)}{EI_b(\xi)} \int_0^\xi R(\theta)\cos\theta d\theta d\xi \right] d\psi \right. \\ &\left. - \sin\phi \int_0^\phi R(\psi)\sin\psi \left[ \frac{\cos\psi}{EA(\psi)} - \frac{\sin\psi}{k_n GA(\psi)} + \int_0^\psi \frac{R(\xi)}{EI_b(\xi)} \int_0^\xi R(\theta)\cos\theta d\theta d\xi \right] d\psi \right\} F_{n_o} \end{aligned} \quad (12)$$

$$\begin{aligned}
w &= \cos \phi w_o + \sin \phi u_o + \left[ \sin \phi \int_0^\phi R(\psi) \cos \psi d\psi - \cos \phi \int_0^\phi R(\psi) \sin \psi d\psi \right] \Omega_{b_o} \\
&+ \left[ \sin \phi \int_0^\phi R(\psi) \cos \psi \int_0^\psi \frac{R(\xi)}{EI_b(\xi)} d\xi d\psi - \cos \phi \int_0^\phi R(\psi) \sin \psi \int_0^\psi \frac{R(\xi)}{EI_b(\xi)} d\xi d\psi \right] M_{b_o} \\
&+ \left\{ \cos \phi \int_0^\phi R(\psi) \left[ \frac{\cos^2 \psi}{EA(\psi)} + \frac{\sin^2 \psi}{k_n GA(\psi)} - \sin \psi \int_0^\psi \frac{R(\xi)}{EI_b(\xi)} \int_0^\xi R(\theta) \sin \theta d\theta d\xi \right] d\psi \right. \\
&+ \left. \sin \phi \int_0^\phi R(\psi) \cos \psi \left[ \frac{\sin \psi}{EA(\psi)} - \frac{\sin \psi}{k_n GA(\psi)} + \int_0^\psi \frac{R(\xi)}{EI_b(\xi)} \int_0^\xi R(\theta) \sin \theta d\theta d\xi \right] d\psi \right\} F_{t_o} \\
&+ \left\{ \cos \phi \int_0^\phi R(\psi) \sin \psi \left[ \frac{\cos \psi}{EA(\psi)} - \frac{\cos \psi}{k_n GA(\psi)} + \int_0^\psi \frac{R(\xi)}{EI_b(\xi)} \int_0^\xi R(\theta) \cos \theta d\theta d\xi \right] d\psi \right. \\
&+ \left. \sin \phi \int_0^\phi R(\psi) \left[ \frac{\sin^2 \psi}{EA(\psi)} + \frac{\cos^2 \psi}{k_n GA(\psi)} - \cos \psi \int_0^\psi \frac{R(\xi)}{EI_b(\xi)} \int_0^\xi R(\theta) \cos \theta d\theta d\xi \right] d\psi \right\} F_{n_o} \quad (13)
\end{aligned}$$

where  $F_{t_o}$  and  $F_{n_o}$  are the internal forces,  $M_{b_o}$  is the internal moment about the bi-normal axis,  $\Omega_{b_o}$  is the rotation angle about the bi-normal axis,  $u_o$  and  $w_o$  are respectively the displacements along the normal and tangential axes of the deformed central line at the reference coordinate  $\phi = \phi_o$  (in this case  $\phi_o = 0$ ).

### 3. The fundamental matrix

The fundamental matrix described in the Eq. (6) can be written in the following expression by using the Eqs. (8)-(13).

$$\begin{bmatrix} w \\ u \\ \Omega_b \\ M_b \\ F_t \\ F_n \end{bmatrix} = \begin{bmatrix} Y_{11} & Y_{12} & Y_{13} & Y_{14} & Y_{15} & Y_{16} \\ Y_{21} & Y_{22} & Y_{23} & Y_{24} & Y_{25} & Y_{26} \\ 0 & 0 & Y_{33} & Y_{34} & Y_{35} & Y_{36} \\ 0 & 0 & 0 & Y_{44} & Y_{45} & Y_{46} \\ 0 & 0 & 0 & 0 & Y_{55} & Y_{56} \\ 0 & 0 & 0 & 0 & Y_{65} & Y_{66} \end{bmatrix} \begin{bmatrix} w_o \\ u_o \\ \Omega_{b_o} \\ M_{b_o} \\ F_{t_o} \\ F_{n_o} \end{bmatrix} \quad (14)$$

The analytical expressions of the fundamental matrix can be calculated easily for any beam with any boundary and loading conditions by using the symbolic calculation tools such as Mathematica, Maple or Mathcad. The program Mathematica is used in this study.

### 3.1 The fundamental matrix of a parabolic beam with variable cross-section

The fundamental matrix for a parabolic beam with variable cross-section is given below. The radius of curvature of the beam, the moment of inertia and the area of the cross-section are respectively given as follows:

$$R(\phi) = R_o/\cos^3 \phi \quad I_b(\phi) = I_{bo}/\cos^3 \phi \quad A(\phi) = A_o/\cos \phi \quad (15)$$

The fundamental matrix is obtained in a simple form:

$$\begin{aligned} Y_{11} &= \cos \phi; & Y_{12} &= \sin \phi; & Y_{13} &= \frac{R_o}{2} \sin \phi \tan \phi; \\ Y_{14} &= \frac{R_o^2}{EI_{bo}} \left[ \left( \frac{\phi \tan \phi + 1}{2} + \log(\cos \phi) \right) \sin \phi - \frac{\phi \cos \phi}{2} \right]; \\ Y_{15} &= R_o(\phi \cos \phi - \log(\cos \phi) \sin \phi) \left( \frac{1}{EA_o} - \frac{1}{k_n GA} + \frac{R_o^2}{2EI_{bo}} \right) + \left( \frac{R_o}{k_n GA} - \frac{R_o^3}{3EI_{bo}} \right) \sin \phi \\ &\quad + \frac{R_o^3}{4EI_{bo}} \left( \frac{\tan \phi}{3} - \phi \right) \sec \phi; \\ Y_{16} &= \frac{R_o^3}{2EI_{bo}} \log(\cos \phi) \sec \phi - R_o(\cos \phi \log(\cos \phi) + \phi \sin \phi) \left( \frac{1}{EA} - \frac{1}{k_n GA} + \frac{R_o^2}{EI_{bo}} \right) \\ &\quad + R_o(\sec \phi - \cos \phi) \left( \frac{1}{EA} + \frac{3R_o^2}{4EI_{bo}} \right); \\ Y_{21} &= -\sin \phi; & Y_{22} &= \cos \phi; & Y_{23} &= \frac{R_o}{2} (\sin \phi + \sec \phi \tan \phi); \\ Y_{24} &= \frac{R_o^2}{4EI_{bo}} \left( \frac{\cos \phi - \sec \phi}{2} + 4(\sec \phi - \sin \phi \tan \phi) \log(\cos \phi) + \sin \phi(3\phi - 3\tan \phi - \phi \tan^2 \phi) \right); \\ Y_{25} &= -R_o(\cos \phi \log(\cos \phi) + \phi \sin \phi) \left( \frac{1}{EA} - \frac{1}{k_n GA} + \frac{R_o^2}{2EI_{bo}} \right) + \frac{R_o^3}{6EI_{bo}} \sec \phi \tan \phi \\ &\quad - \sin \phi \tan \phi \left( \frac{1}{k_n GA} - \frac{R_o^2}{3EI_{bo}} \right); \\ Y_{26} &= R_o(\sin \phi \log(\cos \phi) - \phi \cos \phi) \left( \frac{1}{EA} - \frac{1}{k_n GA} + \frac{R_o^2}{EI_{bo}} \right) + R_o \sin \phi \left( \frac{1}{EA} + \frac{3R_o^2}{4EI_{bo}} \right) \\ &\quad + \frac{R_o^3}{2EI_{bo}} \sec \phi \tan \phi \left( \frac{1}{2} - \log(\cos \phi) \right); \end{aligned}$$

$$\begin{aligned}
Y_{33} &= 1; & Y_{34} &= \frac{R_o \phi}{EI_{bo}}; & Y_{35} &= \frac{R_o^2}{2EI_{bo}}(\tan \phi - \phi); & Y_{36} &= \frac{R_o^2}{EI_{bo}} \log(\cos \phi); \\
Y_{44} &= 1; & Y_{45} &= \frac{1}{2} R_o \tan^2 \phi; & Y_{46} &= -R_o \tan \phi; \\
Y_{55} &= \cos \phi; & Y_{56} &= \sin \phi; & Y_{65} &= -\sin \phi; & Y_{66} &= \cos \phi
\end{aligned} \tag{16}$$

### 3.2 The fundamental matrix of a uniform circular beam

The circular beam with uniform cross-section is widely used in practical applications. The radius of curvature of the beam, the moment of inertia and the area of the cross-section are respectively given as follows:

$$R(\phi) = R_o \quad I_b(\phi) = I_{bo} \quad A(\phi) = A_o \tag{17}$$

The fundamental matrix is obtained in a simple form:

$$\begin{aligned}
Y_{11} &= \cos \phi; & Y_{12} &= \sin \phi; & Y_{13} &= R_o(1 - \cos \phi); & Y_{14} &= \frac{R_o^2}{EI_{bo}}(\phi - \sin \phi); \\
Y_{15} &= \frac{R_o}{2A_o} \left[ \sin \phi \left( \frac{1}{E} - \frac{1}{k_n G} \right) + \phi \cos \phi \left( \frac{1}{E} + \frac{1}{k_n G} \right) \right] + \frac{R_o^3}{2EI_{bo}} \phi (\cos \phi + 2) - \frac{3R_o^3}{2EI_{bo}} \sin \phi; \\
Y_{16} &= \frac{R_o}{2A_o} \phi \sin \phi \left( \frac{1}{E} + \frac{1}{k_n G} \right) + \frac{R_o^3}{2EI_{bo}} (-2 + 2\cos \phi + \phi \sin \phi); \\
Y_{21} &= -\sin \phi; & Y_{22} &= \cos \phi; & Y_{23} &= R_o \sin \phi; & Y_{24} &= \frac{R_o^2}{EI_{bo}}(1 - \cos \phi); \\
Y_{25} &= -\frac{R_o}{2A_o} \phi \sin \phi \left( \frac{1}{E} + \frac{1}{k_n G} \right) + \frac{R_o^3}{2EI_{bo}} (2 - 2\cos \phi - \phi \sin \phi); \\
Y_{26} &= \frac{R_o}{2A_o} \left[ \phi \cos \phi \left( \frac{1}{E} + \frac{1}{k_n G} \right) - \sin \phi \left( \frac{1}{E} + \frac{1}{k_n G} \right) \right] - \frac{R_o^3}{2EI_{bo}} [\phi \cos \phi - \sin \phi]; \\
Y_{33} &= 1; & Y_{34} &= \frac{R_o \phi}{EI_{bo}}; & Y_{35} &= \frac{R_o^2}{EI_{bo}}(\phi - \sin \phi); & Y_{36} &= \frac{R_o^2}{EI_{bo}}[-1 + \cos \phi]; \\
Y_{44} &= 1; & Y_{45} &= R_o(1 - \cos \phi); & Y_{46} &= -R_o \sin \phi; \\
Y_{55} &= \cos \phi; & Y_{56} &= \sin \phi; & Y_{65} &= -\sin \phi; & Y_{66} &= \cos \phi
\end{aligned} \tag{18}$$

### 4. Initial value problem

The solution can be obtained easily in an analytical form, if the initial values are known. Six initial values can be solved from a system of linear equations. These equations can be obtained

from the boundary conditions of the beam.

The conventional boundary conditions are given for the end  $A$  of the beam in Fig. 1:

- i. Clamped end** :  $w(-\phi_A) = 0, \quad u(-\phi_A) = 0, \quad \Omega_b(-\phi_A) = 0$
- ii. Hinged end** :  $w(-\phi_A) = 0, \quad u(-\phi_A) = 0, \quad M_b(-\phi_A) = 0$
- iii. Free end** :  $M_b(-\phi_A) = 0, \quad F_t(-\phi_A) = 0, \quad F_n(-\phi_A) = 0$

When the loads are applied to the free end, the related equations must be equal to the loads. If a beam with point loads at the coordinate ( $\phi = \phi_K$ ) is considered (Fig. 1), there are two regions and the solutions for these regions are:

$$\mathbf{y}_1(\phi_1) = \mathbf{Y}(\phi_1, 0)\mathbf{y}_{1o} \quad \text{for} \quad -\phi_A \leq \phi_1 \leq \phi_K \quad (19)$$

$$\mathbf{y}_2(\phi_2) = \mathbf{Y}(\phi_2, \phi_K)\mathbf{y}_{2K} \quad \text{for} \quad \phi_K \leq \phi_2 \leq \phi_B \quad (20)$$

where  $\mathbf{y}_{2K}$  is the initial value at coordinate  $\phi = \phi_K$  for the second region. The continuity condition at coordinate  $\phi = \phi_K$  is also given as follows:

$$\mathbf{y}_1(\phi_K) + \mathbf{K} = \mathbf{y}_{2K} \quad (21)$$

where  $\mathbf{K} = [0, 0, 0, M_{Kb}, F_{Kt}, F_{Kn}]^T$  is the loading vector. Thus, Eq. (20) is rewritten as:

$$\mathbf{y}_2(\phi_2) = \mathbf{Y}(\phi_2, \phi_K)\mathbf{y}_1(\phi_K) + \mathbf{Y}(\phi_2, \phi_K)\mathbf{K} \quad (22)$$

By substituting Eq. (19) into Eq. (22);

$$\mathbf{y}_2(\phi_2) = \mathbf{Y}(\phi_2, \phi_K)\mathbf{Y}(\phi_K, 0)\mathbf{y}_{1o} + \mathbf{Y}(\phi_2, \phi_K)\mathbf{K} \quad (23)$$

By using Eq. (7), this equation can be given as follows:

$$\mathbf{y}_2(\phi_2) = \mathbf{Y}(\phi_2, 0)\mathbf{y}_{1o} + \mathbf{Y}(\phi_2, 0)\mathbf{Y}^{-1}(\phi_K, 0)\mathbf{K} \quad (24)$$

Then, the analytical functions of the displacements, slope and the stress resultants for both region can be obtained.

Thus, the unknown initial values can be solved by using three simultaneous linear equations for each end. Now, it is possible to specify the displacements, rotation, and internal forces and bending moment of the beam.

## 5. Numerical evaluation

Numerical evaluations are performed for several geometry and boundary and loading conditions. The problems in the literature are also solved and comparisons are made with the results of proposed method.

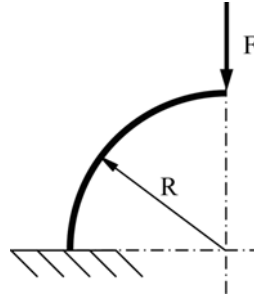


Fig. 2 A quarter-circular cantilever beam loaded by a normal force at the free end

### 5.1 A quarter-circular cantilever beam loaded by a normal force at the free end

As a first example, a quarter-circular cantilever beam with uniform cross-section is studied (Fig. 2). The beam is loaded at the free end by a point force along the normal axis.

The expressions for the displacements and rotation at the free end are obtained as follows:

$$w_o = \frac{FR^3}{2EI_b} + \frac{FR}{2k_nGA} - \frac{FR}{2EA} \quad u_o = \frac{\pi FR^3}{4EI_b} + \frac{\pi FR}{4EA} + \frac{\pi FR}{4k_nGA} \quad \Omega_{bo} = \frac{FR^2}{EI_b} \quad (25)$$

which are the same as those obtained by using Castigliano's energy theorem. This problem has also been considered by several authors (Kim and Kim 1998, Raveendranath *et al.* 1999, Lee and Sin 1994, Ray 2003). Raveendranath *et al.* (1999) and Lee and Sin (1994) give the same analytical expressions, but the sign of the second term in the Eq. (25) of  $w_o$  is minus (-) in (Raveendranath *et al.* 1999, Lee and Sin 1994). It is believed that the source of this difference is a typing error. Several curved beam elements are developed in these studies. Some of the elements have been shown to be free of locking phenomena, and predicting very accurately the displacements and rotations over the wide range of slenderness ratio, while some of them have severe locking phenomenon for thin curved beams.

Very thick beams having  $R/h$  ratios as 1.0, 2.0, and 5.0 are considered in this example. The error is defined as  $e = (w_{os}/w_o - 1)$ , where  $w_{os}$  is the tangential displacement obtained by considering only the shear deformation effect. Similar error definitions are used for other assumptions and the radial displacement  $u_o$ . The error percentage  $e(\%)$  arising from omission of the effects are shown in Table 1.

Table 1 Error percentage arising from omission of the effects

$R/h$	Displacements	No effect $e$ (%)	Only shear $e$ (%)	Only axial $e$ (%)
1	$w_o$	-15.014	7.082	-22.096
	$u_o$	-25.558	-6.203	-19.355
2	$w_o$	-4.230	1.995	-6.225
	$u_o$	-7.905	-1.919	-5.986
5	$w_o$	-0.702	0.331	-1.033
	$u_o$	-1.026	-0.3288	-1.026

The errors decrease, as the ratio of  $R/h$  increases. This means that these effects lose their importance, as the  $R/h$  ratios increase.

The variations along the beam axis of these quantities can be obtained easily:

$$w = \left( -\frac{FR}{2EA} + \frac{FR}{2k_nGA} + \frac{FR^3}{2EI_b} \right) \cos \phi + \left( \frac{FR}{2EA} + \frac{FR}{2k_nGA} + \frac{FR^3}{2EI_b} \right) \left( \frac{\pi}{2} + \phi \right) \sin \phi \quad (26)$$

$$u = \left( \frac{FR}{2EA} + \frac{FR}{2k_nGA} + \frac{FR^3}{2EI_b} \right) \left( \frac{\pi}{2} + \phi \right) \cos \phi \quad (27)$$

$$\Omega_b = \frac{FR^2}{EI_b} \cos \phi \quad (28)$$

## 5.2 Pinched circular ring

The pinched ring problem (Fig. 3) has received considerable attention in recent years due to its practical application. Researchers have studied the pinched ring in order to demonstrate the behavior of their elements in deep beam configurations.

The normal displacement and internal bending moment at the point A are obtained as:

$$u_A = \frac{(\pi^2 - 8)FR^3}{4\pi EI_b} + \frac{\pi FR}{4EA} + \frac{\pi FR}{4k_nGA} \quad M_{bA} = -\frac{2}{\pi}FR \quad (29)$$

The normal displacement and internal bending moment at the point B are given by:

$$u_B = \frac{\pi - 4FR^3}{2\pi EI_b} - \frac{FR}{2k_nGA} + \frac{FR}{2EA} \quad M_{bB} = \left( 1 - \frac{2}{\pi} \right)FR \quad (30)$$

Lee and Sin (1994) solved this problem and the results obtained by Castigliano's theorem were given in analytical forms which are the same as Eqs. (29) and (30). It was shown in Lee and Sin (1994) that the results of the finite element method converged very well.

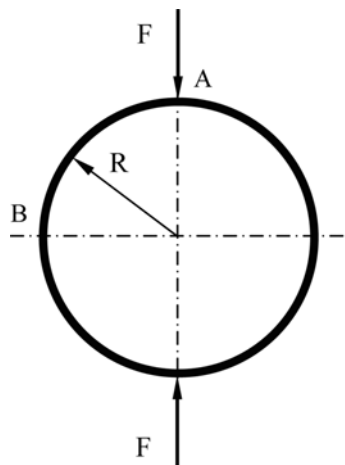


Fig. 3 Pinched ring

Kim and Kim (1998) obtained the solutions for the pinched ring with the radius of curvature  $R=4.953$  in, the thickness of the cross-section  $h=0.094$  in, the width  $b=1$  in, the Young's modulus  $E=1.05 \times 10^6$  lbf/in<sup>2</sup>, the Poisson's ratio  $\nu=0.3125$ , shear distribution factor  $k_n=5/6$  and the load  $F=100$  lbf. The displacement at point A for the ring in Fig. 3 given by Kim and Kim (1998) is  $u_A=1.244$  in. By plugging-in these numerical values in (29), the displacement value is found to be  $u_A=1.24454$  in. Both results are in an excellent agreement.

### 5.3 Nearly straight beam

A beam having very large radius and short span is considered by several authors (Kim and Kim 1998, Raveendranath *et al.* 1999, Ray 2003) to test the accuracy of their beam finite elements and to investigate the possibility of approximating to straight beam configurations by using the curved beam finite elements. Fig. 4 shows the geometry of a thin nearly straight cantilever beam subjected to a tip force. The length of the beam is  $L=10$  in, the width and thickness of the cross-section are respectively  $b=1$  in and  $h=0.01$  in, and the radius of curvature is  $R=10000$  in. The material properties are  $E=10^7$  lbf/in<sup>2</sup>,  $\nu=0.3$  and the shear correction factor is  $k_n=5/6$ . A unit vertical load is applied to the free end. The displacements, rotation angle, bending moment, and shear and axial forces are calculated for several points  $s/L$ , where  $s$  is the curvilinear coordinate along the arch axis. The results are given in Table 2. The finite elements developed by Kim and Kim (1998), Raveendranath *et al.* (1999) and Ray (2003) predict very accurately the exact solutions given in Table 2.

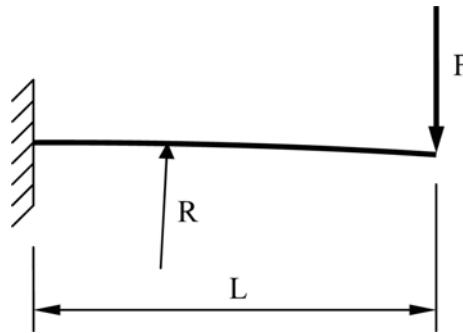


Fig. 4 Nearly straight cantilever beam

Table 2 The results of nearly straight cantilever beam

$s/L$	$w$ (in)	$u \times 10^{-3}$ (in)	$\Omega_b \times 10^{-2}$ (rad)	$M_b$ (lbf.m)	$F_n$ (lbf)	$F_t$ (lbf)
1.00	0.14902	0.400	0.60	0	0	1.0
0.75	0.0685546	0.253	0.5625	2.5	$0.25 \times 10^{-3}$	1.0
0.50	0.0217773	0.125	0.45	5	$0.5 \times 10^{-3}$	1.0
0.25	0.002832	0.0343751	0.2625	7.5	$0.75 \times 10^{-3}$	1.0
0.00	0.0	0.0	0.0	10	$1 \times 10^{-3}$	1.0

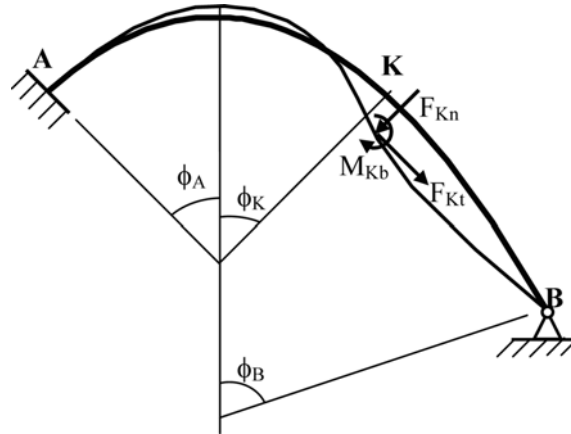


Fig. 5 Clamped-hinged unsymmetrical parabolic beam

#### 5.4 Parabolic beam with unsymmetrical boundary and loading conditions

Unsymmetrical parabolic beam with uniform cross-section is hinged at one end and clamped at the other end (Fig. 5). The angles in this figure are  $\phi_A = -45^\circ$ ,  $\phi_K = 45^\circ$ ,  $\phi_B = 63.435^\circ$ . The tangential and normal forces and bending moment are applied to the point K. Consider a beam having the following parameters: The dimensions of the cross-section are  $b = 0.01$  m and  $h = 0.015$  m, and the radius of curvature at  $\phi = 0$  is  $R_o = 0.1$  m. The radius of curvature for a parabolic beam is known as  $R(\phi) = R_o/\cos^3 \phi$ . The material properties are  $E = 2 \times 10^{11}$  N/m<sup>2</sup> and  $\nu = 0.3$ . The loads are  $F_{Kn} = 500$  N,  $F_{Kt} = 500$  N,  $M_{Kb} = 1000$  Nm and  $k_n = 5/6$ . The solutions for the midpoint are as follows:

$$\begin{aligned} w_o &= -0.314 \text{ mm}, & u_o &= -0.765 \text{ mm}, & \Omega_{bo} &= -7.364 \times 10^{-3} \text{ rad}, \\ M_{bo} &= 94.5545 \text{ Nm}, & F_{to} &= 1274.13 \text{ N}, & F_{no} &= -2899.53 \text{ N} \end{aligned}$$

The deformed shape of the beam is also given in Fig. 5.

#### 5.5 Cantilever beams having spiral geometry with variable cross-section

Consider a spiral beam defined by the cylindrical coordinate  $r = R_o (1 - \mu \theta)$ , where  $\mu$  is a constant and  $\theta$  is the angular coordinate ( $0 \leq \theta \leq \pi/2$ ) (Fig. 6). The circular geometry is obtained when  $\mu = 0$ . The cross-section varies along the beam and functions for the area and moment of inertia terms are assumed to be:

$$A = A_o (1 + \alpha \Theta)^2 \quad I_b = I_{bo} (1 + \alpha \Theta)^4 \quad (31)$$

where  $A_o$  and  $I_{bo}$  are the area and moment of inertia of the cross-section at  $\theta = 0^\circ$  respectively, and  $\Theta = \theta/(\pi/2)$  is the normalized angular coordinate. The beam is clamped at  $\theta = \pi/2$  and a point force  $F = 1000$  N is applied at its free end ( $\theta = 0^\circ$ ). The uniform cross-section is obtained when  $\alpha = 0$ . Numerical values are chosen as follows:

$$R_o = 1 \text{ m}, A_o = 0.01 \text{ m}^2, I_{bo} = 8.333 \times 10^{-6} \text{ m}^4, E = 2 \times 10^{10} \text{ N/m}^2, \nu = 0.15 \text{ and } k_n = 5/6$$

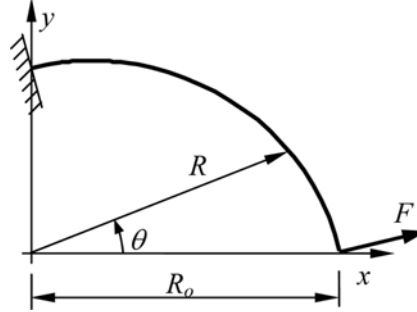


Fig. 6 Cantilever curved beam having spiral geometry

Table 3 gives the solutions for circular beams ( $\mu = 0.0$ ) with  $\alpha = 0, 0.2$  and  $0.4$ . Table 4 gives the solutions for spiral beams ( $\mu = 0.4$ ) with  $\alpha = 0, 0.2$  and  $0.4$ .

The aim of the example is to show that the exact solutions can be obtained for a curved beam having variable curvature and variable cross-section. As far as the authors know, there is no curved beam finite element with variable cross-section.

### 5.6 The effects of axial extension and shear deformation

In this section, the effects of axial extension and shear deformation are studied. For this purpose, the examples in the study of Litewka and Rakowski (1998) are solved and the results are compared with each other. The thick arch finite element was developed by using the exact stiffness matrix for shear-flexible and compressible element in Litewka and Rakowski (1998). The beam with radius of curvature  $R = 4$  m, the rectangular cross-section with depth  $h = 0.6$  m and width  $b = 0.4$  m, the opening angle  $\phi_i = 2\pi/3$ , Young's modulus  $E = 30$  GPa and Poisson's ratio  $\nu = 0.17$  with different boundary conditions and loading is investigated by taking into account the effects of axial extension and shear deformation. The loads are  $F = 1$  kN and  $M = 1$  kNm. The normalized vertical displacement  $u/(R\phi_i)$  and the normalized slope  $\Omega_b/\phi_i$  of the beam at the midpoint were obtained by including or excluding the axial extension and shear deformation effects in the analyses. The following parameters were defined in order to include these effects:

$$d = \frac{EI}{k_n GA} \frac{1}{(R\phi_i)^2} = 0.0192 \quad e = \frac{EI}{EA} \frac{1}{(R\phi_i)^2} = 0.00684 \quad (30)$$

Most of the examples given by Litewka and Rakowski (1998) are solved and the results of both studies are given in Table 5. The comparison shows that the finite element developed by Litewka and Rakowski (1998) predicts accurately the displacement and slope at the midspan. It can also be seen that the axial extension is the major effect. There are very large differences between the results obtained by considering both axial extension and shear deformation effects and those obtained by neglecting them. This shows that the Euler-Bernoulli beam theory gives acceptable results for only a slender and deep curved beam where the bending deformation is the main effect. Moreover, when the beam is stubby, the shear deformation effect becomes significant.

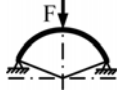
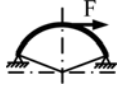
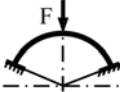
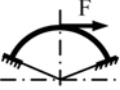
Table 3 Displacements, slopes, bending moment and internal forces at different points for cantilever circular beams ( $\mu = 0.0$ ) with uniform ( $\alpha = 0.0$ ) and non-uniform cross-sections ( $\alpha = 0.2$  and  $0.4$ )

$\alpha$		$\phi$									
		0°	10°	20°	30°	40°	50°	60°	70°	80°	90°
0.0	$w$ (cm)	0.189998	0.137196	0.093646	0.05956	0.034511	0.017517	0.007225	0.002025	$1.918 \times 10^{-4}$	0
	$u$ (cm)	0.315417	0.265645	0.212845	0.160706	0.11112	0.063043	0.012095	-0.04814	-0.12291	0
	$\Omega_b \times 10^{-3}$ (rad)	4.56325	4.47162	4.21192	3.80982	3.2936	2.6927	2.03636	1.35242	0.666261	0
0.2	$w$ (cm)	0.109929	0.077895	0.052100	0.032440	0.018385	0.009118	0.003664	$9.88 \times 10^{-4}$	$7.912 \times 10^{-5}$	0
	$u$ (cm)	0.193359	0.159267	0.124376	0.091259	0.060724	0.031237	$-9.7 \times 10^{-4}$	-0.04057	-0.090792	0
	$\Omega_b \times 10^{-3}$ (rad)	2.94581	2.85936	2.63248	2.30919	1.92698	1.51674	1.10296	0.704194	0.333677	0
0.4	$w$ (cm)	0.069048	0.048069	0.031557	0.019279	0.010718	0.005210	0.002046	$5.32 \times 10^{-4}$	$3.352 \times 10^{-5}$	0
	$u$ (cm)	0.01279	0.103124	0.078602	0.056164	0.036001	0.016469	0.005577	-0.03362	-0.069689	0
	$\Omega_b \times 10^{-3}$ (rad)	2.04705	1.96538	1.76616	1.50311	1.21396	0.924257	0.650503	0.402485	0.185145	0
Any $\alpha$	$M_b$ (Nm)	0	-174.053	-336.658	-483.008	-609.157	-712.122	-789.945	-841.723	-867.585	-868.638
	$F_t$ (N)	0	180.484	355.507	519.263	666.226	791.326	890.111	958.893	994.879	996.274
	$F_n$ (N)	-1000	-983.578	-934.674	-854.615	-745.75	-611.394	-455.744	-283.769	-101.076	86.2417

Table 4 Displacements, slopes, bending moment and internal forces at different points for cantilever spiral beams ( $\mu = 0.4$ ) with uniform ( $\alpha = 0.0$ ) and non-uniform cross-sections ( $\alpha = 0.2$  and  $0.4$ )

$\alpha$		$\phi$									
		0°	10°	20°	30°	40°	50°	60°	70°	80°	90°
0.0	$w$ (cm)	0.145342	0.103104	0.06910	0.043164	0.024579	0.012274	0.004982	0.001369	$1.22 \times 10^{-4}$	0
	$u$ (cm)	0.232792	0.189071	0.145379	0.104647	0.067087	0.029239	-0.01517	-0.07137	-0.13739	0
	$\Omega_b \times 10^{-3}$ (rad)	3.78636	3.68693	3.41622	3.017	2.53163	1.99965	1.45571	0.928186	0.43832	0
0.2	$w$ (cm)	0.086053	0.059674	0.039029	0.023769	0.013187	0.006409	0.002523	$6.63 \times 10^{-4}$	$4.74 \times 10^{-5}$	0
	$u$ (cm)	0.147143	0.116444	0.086847	0.060353	0.036502	0.012052	-0.01793	-0.05697	-0.10294	0
	$\Omega_b \times 10^{-3}$ (rad)	2.50942	2.41561	2.17903	1.85793	1.49843	1.13508	0.792004	0.484289	0.219634	0
0.4	$w$ (cm)	0.055117	0.037421	0.023935	0.01425	0.007728	0.003668	0.001405	$3.52 \times 10^{-4}$	$1.78 \times 10^{-5}$	0
	$u$ (cm)	0.099848	0.077088	0.055877	0.037581	0.021397	0.004416	-0.01727	-0.04610	-0.08005	0
	$\Omega_b \times 10^{-3}$ (rad)	1.78228	1.69363	1.48583	1.22448	0.95241	0.695735	0.468674	0.277214	0.12191	0
Any $\alpha$	$M_b$ (Nm)	0	-181.149	-344.345	-484.128	-596.488	-678.976	-730.75	-752.55	-746.608	-716.488
	$F_t$ (N)	0	198.809	392.867	574.1	734.061	864.006	954.964	997.842	983.648	904.081
	$F_n$ (N)	-1000	-980.038	-919.596	-818.785	-679.083	-503.482	-296.722	-65.6655	180.1	427.362

Table 5 The results of Litewka and Rakowski (1998) (L&R) and this study for the normalized vertical displacement  $u_o/(R\phi_T)$  and normalized rotation  $\Omega_{bo}/\phi_T$  of four different problems

		$\times 10^{-6}$	All Effects	Axial Ext.	Shear Def.	No Effect
	$\frac{u_o}{R\phi_T}$	L&R	0.3047	0.2546	0.2010	0.1748
		This Study	0.280916	0.254627	0.201031	0.17471
	$\frac{u_o}{R\phi_T}$	L&R	0.2884	0.2770	0.2460	0.2348
		This Study	0.28831	0.277106	0.24606	0.234814
	$\frac{\Omega_{bo}}{R\phi_T}$	L&R	-0.8064	-0.8122	-0.8274	-0.8332
		This Study	-0.806359	-0.811982	-0.827505	-0.833128
	$\frac{u_o}{R\phi_T}$	L&R	-0.2016	-0.2030	-0.2069	-0.2083
		This Study	-0.20159	-0.202996	0.206876	0.208282
	$\frac{\Omega_{bo}}{\phi_T}$	L&R	1.3613	1.3383	1.3579	1.3350
		This Study	1.36129	1.33832	1.35789	1.33493
	$\frac{u_o}{R\phi_T}$	L&R	0.2488	0.2205	0.1430	0.1127
		This Study	0.248781	0.220506	0.143015	0.112688
	$\frac{u_o}{R\phi_T}$	L&R	0.1252	0.1136	0.0889	0.0773
		This Study	0.12522	0.113602	0.0888806	0.773037
	$\frac{\Omega_{bo}}{\phi_T}$	L&R	-0.3796	-0.3683	-0.4063	-0.3952
		This Study	-0.3796417	-0.368286	-0.406268	-0.395228
	$\frac{u_o}{R\phi_T}$	L&R	-0.0949	-0.0921	-0.1016	-0.0988
		This Study	-0.09491	-0.09207	0.101567	0.098807
	$\frac{\Omega_{bo}}{\phi_T}$	L&R	1.0824	1.0375	1.0757	1.0304
		This Study	1.08224	1.03731	1.07567	1.03057

### 5.7 Comparison of the results for deep and shallow curved beams

The Euler beam theory gives acceptable results for a slender and deep curved beam where the bending deformation is the main effect. But the results are not reasonable when the curved beam is shallow. The axial extension is an important effect for a shallow curved beam, even if it is slender. As it is well known, when the beam is stubby, the shear deformation effect becomes significant.

Deep and shallow curved beams exhibit different static and dynamic behavior (Tufekci 2001,

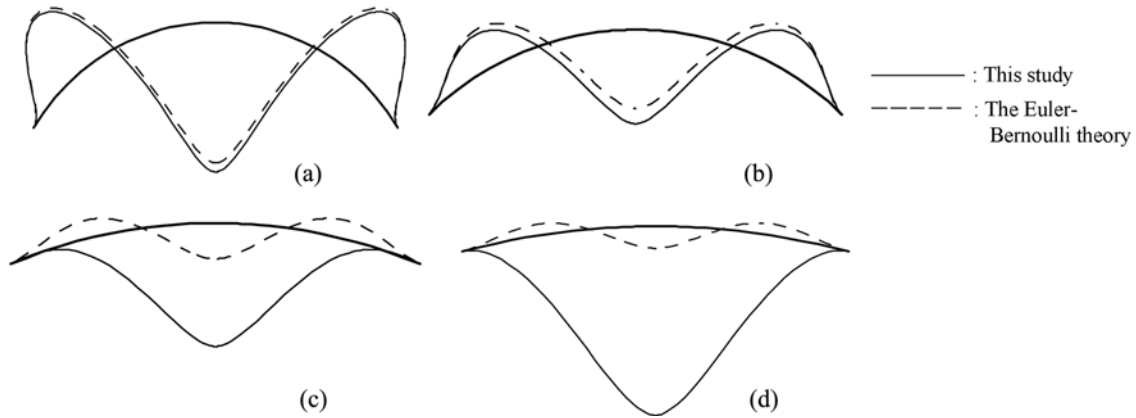


Fig. 7 The deformations of the circular beams with opening angles of (a)  $\phi_i = 120^\circ$ , (b)  $\phi_i = 90^\circ$ , (c)  $\phi_i = 45^\circ$ , (d)  $\phi_i = 30^\circ$  (clamped at both ends and under a vertical force at the midpoint)

Rubin 2004). A shallow curved beam deforms along a different path representing another characteristic deformed shape.

In order to exhibit the effect of the shallowness of a curved beam, a numerical example is given in this section. A circular beam with clamped ends is considered here. The beam is loaded by a force at the midspan. The cross-section of the beam is rectangular. The slenderness ratio of the beam is  $R/\sqrt{IA} = 100$ . Fig. 7 shows the deformation of the circular beams with several opening angles. The dashed lines show the results of Euler-Bernoulli beam theory; the solid lines show the results of this study which considers the effects of axial extension and shear deformation. As it can be seen from the figure, the difference between the results of Euler-Bernoulli theory (dashed line) and this study (solid line) are less than 10% for  $\phi_i = 120^\circ$  (Fig. 7a); the difference between these solutions increases, when the opening angle decreases. For  $\phi_i < 45^\circ$  (Fig. 7c), it is not only the displacements at the crown are different, but also the deformed shape is different. The effect of axial extension is significant for a shallow curved beam even if it is slender. The effect of shear deformation is also important when the beam is thick, as it is expected. The shallow beam with opening angle of  $30^\circ$  is still slender in this example; and the deformed shape is given in Fig. 7(d).

## 6. Conclusions

The approximate methods excluding finite element method are only useful in solving the simple problems in which the effects of the axial extension, shear deformation or both are neglected. Also, the formulation has to be done separately for each problem because the chosen displacement functions depend on the boundary conditions and axis geometry of the beam.

The finite element method has widely been used in literature for analyzing the curved beams. Special beam elements for curved geometry have been developed recently. Early formulations of curved finite beam elements were not successful due to the element locking problems. Much attention has been devoted to solve the locking problems over the years. Most of the elements have been developed for the circular beams having uniform cross-sections. As far as the authors know,

there is no curved beam finite element with variable cross-section. The finite element method solves the problems of curved beams with variable cross-section by using piecewise constant cross-section beam elements to approximate the variable cross-section beam. Motivated by this fact, the exact solution is developed to solve the static problems of planar curved beams with variable cross-section and variable curvature by taking into account the axial extension and shear deformation effects. The exact solution is obtained by using the initial values method by which the displacements, rotation and stress resultants can be calculated analytically along the beam axis. An advantage of this method is that the high degree of statically indeterminacy adds no extra difficulty to the solution of problems. The fundamental matrix, which is necessary to apply the initial values method, is obtained analytically. An example for this matrix is given explicitly. The analytical expressions of the fundamental matrix can be obtained as long as the integrals can be calculated analytically by using symbolic calculation tools such as Mathematica, Mathcad or Maple.

Main contribution of this study is to give the exact solutions for the curved beams with varying curvature and cross-section. The results of the proposed method do not depend on the geometry. The exact solution can be obtained for all geometric types of beam axes and all doubly symmetric variable cross-sections. The accuracy of the results does not depend on the slenderness ratio and the shallowness of the beam. The results for several sample problems are presented by considering the axial extension and shear deformation effects.

## Acknowledgements

The authors are greatly indebted to the late Professor Dr. Vural Cinemre of Istanbul Technical University for his appreciable enlightenment and overall guidance. Prof. Dr. Mustafa Savci at Istanbul Technical University is acknowledged with gratitude for his valuable encouragement and support. The authors would also like to acknowledge Assoc. Prof. Ata Mugan from Istanbul Technical University for helpful discussions.

## References

- Antman, S.S. (1972), "The theory of rods", 641-703, in: C. Truesdell (Ed.), *Handbuch der Physik*, Vol. VI a/2, Springer Verlag, Berlin.
- Asplund, S.O. (1961), "Deflection theory of arches", *J. Struct. Div.*, ASCE, **87**, ST7, 125-149.
- Atluri, S.N., Iura, M. and Vasudevan, S. (2001), "A consistent theory of finite stretches and finite rotations in space-curved beams of arbitrary cross-section", *Comput. Mech.*, **27**, 271-281.
- Benlemlih, A. and El Ferrichia, M.E.A. (2002), "A mixed finite element method for the arch problem", *Appl. Math. Model.*, **26**, 17-36.
- Cinemre, V. (1982), "Strain-displacement relations in rod theory", *ITU Dergisi*, **40**, 1-6, (In Turkish).
- Dawe, D.J. (1974), "Curved finite elements for the analysis of shallow and deep arches", *Comput. Struct.*, **4**, 559-580.
- Huddleston, J.V. (1968), "Finite deflections and snap-through of high circular arches", *J. Appl. Mech.*, **35**(4), 763-769.
- Kapania, R.K. and Li, J. (2003), "A formulation and implementation of geometrically exact curved beam elements incorporating finite strains and finite rotations", *Comput. Mech.*, **30**, 444-459.
- Kim, J.G. and Kim, Y.Y. (1998), "A new higher-order hybrid-mixed curved beam element", *Int. J. Numer. Meth. Eng.*, **43**, 925-940.

- Lee, P-G and Sin, H-C. (1994), "Locking-free curved beam element based on curvature", *Int. J. Numer. Meth. Eng.*, **37**, 989-1007.
- Litewka, P. and Rakowski, J. (1998), "The exact thick arch finite element", *Comput. Struct.*, **68**, 369-379.
- Love, A.E.H. (1944), *A Treatise on the Mathematical Theory of Elasticity*, Dover Publication, New York.
- Raveendranath, P., Singh, G. and Pradhan, B. (1999), "Two-noded locking-free shear flexible curved beam element", *Int. J. Numer. Meth. Engng.*, **44**, 265-280.
- Ray, D. (2003), "c-type method of unified CAMG and FEA. Part 1: Beam and arch mega-elements-3D linear and 2D non-linear", *Int. J. Numer. Meth. Engng.*, **58**, 1297-1320.
- Reissner, E. (1972), "On one-dimensional finite strain beam theory: The plane problem", *J. Appl. Math. Phys. (ZAMP)*, **23**, 795-804.
- Reissner, E. (1973), "On one-dimensional large displacement finite strain beam theory", *Stud. Appl. Math.*, **52**, 87-95.
- Rubin, M.B. (2000), *Cosserat Theories: Shells, Rods and Points*, Kluwer Academic Publishers, The Netherlands.
- Rubin, M.B. (2004), "Buckling of elastic shallow arches using the theory of cosserat point", *J. Eng. Mech.*, **130**(2), 216-224.
- Schulz, M. and Filippou, F.C. (2001), "Non-linear spatial Timoshenko beam element with curvature interpolation", *Int. J. Numer. Meth. Eng.*, **50**, 761-785.
- Stolarski, H. and Belytschko, T. (1983), "Shear and membrane locking in curved  $C^0$  elements", *Comput. Meth. Appl. Mech. Eng.*, **41**, 279-296.
- Tessler, A. and Spiridigliozzi, L. (1986), "Curved beam elements with penalty relaxation", *Int. J. Numer. Meth. Eng.*, **23**, 2245-2262.
- Tufekci, E. and Arpacı, A. (1998), "Exact solution of in-plane vibrations of circular arches with account taken of axial extension, transverse shear and rotatory inertia effects", *J. Sound Vib.*, **209**, 845-856.
- Tufekci, E. (2001), "Exact solution of free in-plane vibration of shallow circular arches", *Int. J. Struct. Stab. Dynam.*, **1**, 409-428.